

On the Luminosity of Young Jupiters

Mark S. Marley

NASA Ames Research Center; Mail Stop 245-3; Moffett Field CA 94035

Mark.S.Marley@NASA.gov

Jonathan J. Fortney

*Spitzer Fellow, NASA Ames Research Center; Mail Stop 245-3; Moffett Field CA 94035
and SETI Institute, 515 N. Whisman Rd., Mountain View, CA 94043*

jfortney@mail.arc.nasa.gov

Olenka Hubickyj

NASA Ames Research Center; Mail Stop 245-3; Moffett Field CA 94035

Peter Bodenheimer

UCO/Lick Observatory, University of California, Santa Cruz CA 95064

and

Jack J. Lissauer

NASA Ames Research Center; Mail Stop 245-3; Moffett Field CA 94035

ABSTRACT

Traditional thermal evolution models of giant planets employ arbitrary initial conditions selected more for computational expediency than physical accuracy. Since the initial conditions are eventually forgotten by the evolving planet, this approach is valid for mature planets, if not young ones. To explore the evolution at young ages of jovian mass planets we have employed model planets created by one implementation of the core accretion mechanism as initial conditions for evolutionary calculations. The luminosities and early cooling rates of young planets are highly sensitive to their internal entropies, which depend on the formation mechanism and are highly model dependent. As a result of the accretion shock through which most of the planetary mass is processed, we find lower initial internal entropies than commonly assumed in published evolution

tracks. Consequently young jovian planets are smaller, cooler, and several to 100 times less luminous than predicted by earlier models. Furthermore the time interval during which the young jupiters are fainter than expected depends on the mass of planet. Jupiter mass planets ($1 M_J$) align with the conventional model luminosity in as little as 20 million years, but $10 M_J$ planets can take up to 1 billion years to match commonly cited luminosities, given our implementation of the core accretion mechanism. If our assumptions, especially including our treatment of the accretion shock, are correct and if extrasolar jovian planets indeed form with low entropy, then young jovian planets are substantially fainter at young ages than currently believed. Furthermore early evolution tracks should be regarded as uncertain for much longer than the commonly quoted 10^6 years. These results have important consequences both for detection strategies and for assigning masses to young jovian planets based on observed luminosities.

Subject headings: planets and satellites: formation; (stars:) planetary systems: formation; stars: individual (2MASSWJ1207334-393254b, GQ Lup b); planets: individual (HD 209458 b)

1. Introduction

In the past decade, a number of nearby star associations have been recognized as being quite young, less than 10 Myr old (e.g. IC 348, TW Hydrae, MBM12, η Cha (Lada & Lada 1995; Webb et al. 1999; Luhman & Steeghs 2004)). Such associations are likely well stocked with recently formed, presumably bright giant planets that should in principle be easy prey for a variety of planet detection technologies. Planning for the hunt, however, requires knowledge of the expected luminosity of young giant planets as a function of time since their formation, particularly at young ages when they are presumably easy game.

While models of the luminosity evolution of giant planets have a long pedigree (e.g., Grossman et al. 1972; Graboske et al. 1975), the early work focused on the evolution of the solar system giants, attempting to explain their current luminosity at an age of 4.5 Gyr. Since planets lose memory of their initial conditions over time, initial conditions were selected more for computational convenience than for accuracy. Many improvements have subsequently been made to the models, particularly in the characterization of jovian atmospheres at various effective temperatures, although essentially the same initial conditions are still employed (Hubbard 1980; Burrows et al. 1997; Chabrier et al. 2000).

The standard evolution model begins with a hydrogen-helium sphere having a large

radius, high internal entropy, and large effective temperature. Such an object is not necessarily one that would be the result of any particular planet formation model. This model planet is allowed to radiate and cool over time. Since there have been no detections yet of young planets with measured masses, the applicability of this initial condition is untested, although there are data from more massive objects. A pair of eclipsing, young (~ 1 Myr) brown dwarfs with known dynamical masses (57 and 36 Jupiter masses (M_J)) indeed have radii exceeding five times that of Jupiter (Stassun et al. 2006), confirming that young massive brown dwarfs, at least, are in fact large and hot. But giant planets that formed in a disk around a primary star, or even isolated planet-mass objects, may have experienced very different initial conditions.

Evolution tracks computed in the usual way—even though they do not necessarily reflect any particular planet formation theory—have been used to evaluate detection strategies for true giant planets orbiting solar type stars (e.g., Burrows 2005), and they have been used to characterize isolated, very low mass brown dwarfs. Chauvin et al. (2004), for example, reported on the detection of a faint companion to the M8 brown dwarf 2MASSWJ1207334-393254 (hereafter 2MASS1207) in TW Hydrae with an estimated age of 8 Myr. Using its observed luminosity and applying published evolution tracks, they estimated a mass of just $5 M_J$ for the mass of the companion.

The early modelers certainly did not foresee that direct detections of putative young planets would be compared against the models at exceptionally young ages, at times when the model planet may not yet have forgotten its hot start. Stevenson (1982) wrote that evolution calculations “...cannot be expected to provide accurate information on the first 10^5 – 10^8 years of evolution because of the artificiality of an initially adiabatic, homologously contracting¹ state.” More recently, Baraffe et al. (2002) examined the uncertainties in evolution tracks of brown dwarfs at young ages and cautioned about the applicability of evolution models at ages less than a few million years, on the lower end of Stevenson’s uncertainty range. Wuchterl (2005) has also expressed concern that standard evolution models do not capture the early evolution correctly. Given the clear imperatives to interpret observations of young, low mass objects and to plan for future direct detections of giant planets formed in orbit about solar type stars, there is a need to connect models of giant planet formation to giant planet evolution.

Our goals here are both to help fill the void in physically plausible models of extrasolar giant planets (EGPs) at young ages and to better quantify the age beyond which the evolution models are robust and applicable. We aim to understand whether or not the current

¹See Stahler (1988) for a discussion of homologous contraction.

generation of evolution models can reliably predict the luminosity of giant planets at young ages and, if not, then define the age beyond which current models are reliable. Instead of using an arbitrary starting condition, we employ planets formed by one implementation of the core accretion model. In this scenario gas giant planets form by rapid accretion of gas onto a solid core that grew by accretion of planetesimals in the nebula. This mechanism is one of two competing scenarios of gas giant formation, the other being the gas instability model by which giants form from a local disk instability (Boss 1998) that creates a self-gravitating clump of gas. The planet resulting from such a clump could also be used as the starting point of an evolutionary calculation (see Bodenheimer (1974, 1976); Bodenheimer et al. (1980)), but we choose here to focus solely on the core accretion mechanism as it currently seems the more promising mechanism for explaining the formation of the giant planets (see Lissauer & Stevenson (2006) for a review).

For specificity, we rely upon the implementation by Hubickyj et al. (2005) of the core accretion mechanism. By necessity, their work makes a host of assumptions that ultimately affect the properties of newly born giant planets. As we will demonstrate, following the end of accretion this model predicts that giant planets are substantially fainter than standard evolution models. While we believe that this conclusion is secure, we stress that the precise numerical value of the post-accretion luminosity depends upon the particular assumptions employed by Hubickyj et al. (2005). Therefore, we first briefly review this model and highlight the assumptions upon which the work rests in Section 2. We describe our method of evolving these model planets over time in Section 3 and compare our results with standard giant planet evolution models. We find in Section 4 that the initial conditions influence subsequent planetary evolution for longer than generally appreciated and that planets formed by the Hubickyj et al. (2005) recipe for core accretion are substantially fainter than standard models have previously predicted. We end by cautioning those who wish to rely upon evolution models to characterize detected young giant planets that may have grown by the core accretion mechanism would be wise to be judicious in their estimation of the model-dependent uncertainties.

2. Accretion

The core accretion model describing the formation of giant planets (Mizuno 1980; Bodenheimer & Pollack 1986; Pollack et al. 1996) suggests that any planet that becomes more massive than about $10 M_{\oplus}$ (Earth masses) while residing within a gas-rich protoplanetary nebula should accrete a gaseous envelope. This leads to the expectation that massive planets acquire a thick envelope of roughly nebular composition surrounding a denser core of rock

and ice. In this section, we briefly review the particular implementation of this model by Pollack et al. (1996) and collaborators (Bodenheimer et al. 2000; Hubickyj et al. 2005) and inform the reader of important model assumptions. The newborn planets delivered by this modeling approach are then used as initial conditions to our own evolution calculations as described in Section 3.

2.1. Model Overview

Bodenheimer et al. (2000) describe the core accretion-gas capture process. The stages described below are chosen for clarity, and do not match the accretion phases as defined in Bodenheimer et al. (2000). Each stage is keyed to Figure 1, which illustrates the luminosity evolution of an accreting $1 M_J$ planet.

1. Dust particles in the solar nebula form planetesimals that accrete into a solid core surrounded by a very low-mass gaseous envelope. During runaway solid accretion the gas accretion rate is much lower than that of solids. As the solid material in the feeding zone is depleted, the solid mass accretion rate and consequently the luminosity fall. At the end of this stage, most of the mass of the planet consists of solids.
2. The protoplanet continues to grow as the gas accretion rate steadily increases, eventually exceeding the solids accretion rate. The mass of both components grow until the core and envelope masses become equal.
3. Runaway gas accretion occurs and the protoplanet grows rapidly. The evolution up to this point is referred to as the *nebular stage*, because the outer boundary of the protoplanetary envelope is in contact with the solar nebula and the density and temperature at this interface merge with nebular values. During this stage, the nebula is assumed to provide the planet with enough mass that the planet always fills its effective accretion radius, which is almost as large as the radius of its Hill sphere (Bodenheimer et al. 2000)².
4. As the planet grows, its hunger for gas increases, however the rate of gas consumption is limited to the rate at which the nebula can transport gas to the vicinity of the planet. Subsequently, the region of the protoplanet in hydrostatic equilibrium contracts inside the effective accretion radius (which at this time is close to that of the Hill sphere), and gas accretes hydrodynamically onto the planet. Note that the $1 M_J$ accretion model we employ is that of Hubickyj et al. (2005). For the more massive planets, we allow this $1 M_J$ model

²The core continues to grow during this time as large planetesimals are accreted. Final core masses range from 17 to $19 M_\oplus$ for our 1 and $10 M_J$ models, respectively.

to spend more time in this phase, with a gas accretion rate $\dot{M}_{\text{gas}} \approx 10^{-2} M_{\oplus} \text{ yr}^{-1}$, until the planet reaches its final target mass. Accretion is stopped by either the opening of a gap in the disk as a consequence of accretion, the tidal effect of the planet, by dissipation of the nebula, or some combination of all three. For computational stability, \dot{M}_{gas} is linearly decreased from the limiting rate to zero over a time period of $3.5 \times 10^4 \frac{M}{1 M_{\text{J}}} \text{ yr}$, where M is the mass of the planet.

During this time of rapid gas accretion, the accreting gas is assumed to fall from the Hill sphere radius down to the surface of the planet. It arrives at a shock interface where almost all of the initial gravitational potential energy of the gas is radiated away upwards, as occurs for accreting stars (Stahler et al. 1980). This produces a rapid increase in luminosity and the planet briefly shines quite brightly. *Crucial to the problem at hand is that the gas arrives at the surface of the planet having radiated away most of its gravitational potential energy and initial specific entropy and having equilibrated with the local thermal radiation field.*

5. Once accretion stops, the planet enters the isolation stage. During this stage the planet contracts and cools to the present state at constant mass. The details of our calculation of the planet’s evolution are presented in the Section 3.

2.2. Important Model Assumptions

Detailed descriptions of the procedure and assumptions that enter into the implementation of the core accretion model are reported in Pollack et al. (1996), Bodenheimer et al. (2000), and Hubickyj et al. (2005). For this study we prepared core accretion models for masses of 2, 4, 6, 8, and 10 M_{J} by starting with the 1 M_{J} baseline case (denoted 10L ∞) from Hubickyj et al. (2005). For simplicity, we assumed Stages 1 through 3 to be identical for all planetary masses and only the total duration of Stage 4 controls the final mass of the planet. The special cases (e.g., the high nebular temperature case) are new models, computed in the same way as the others, except for the one changed parameter.

The protoplanet grows as a lone embryo in a solar nebula of a temperature $T_{\text{neb}} = 150 \text{ K}$ and density $\rho_{\text{neb}} = 5 \times 10^{-11} \text{ g cm}^{-3}$ with a protosolar hydrogen to helium ratio. The planetesimal feeding zone, which is assumed to be an annulus extending to a radial distance of about 4 Hill-sphere radii on either side of the planet’s orbit, grows as the planet gains mass. It is assumed that gas from the surrounding solar nebula flows freely, up to a limiting rate, into the evacuated volume.

The atmospheric boundary condition for the entire core accretion evolution relies upon a

gray atmosphere computed with Rosseland mean opacities. This mean opacity is controlled by the assumed grain number density and size distribution of particles arriving from the nebula. We employ the ‘L’ models of Hubickyj et al. (2005) in which the opacity due to grains is 2% of the interstellar grain opacity. This grain opacity is in agreement with computations by Podolak (2003) that indicate that when the grains enter the protoplanetary envelope, they coagulate and settle out quickly into warmer regions where they are destroyed, resulting in actual opacities in this low temperature region far smaller than interstellar values. Nonetheless, throughout the relevant effective temperature range grain opacity dominates the pure gaseous opacity.

During stage 3, the gas accretion rate increases very quickly. We limit this increase to the rate at which the solar nebular can supply gas to the planet. Typical protoplanetary nebula models state that the mass transfer rate, caused by viscous effects, is about $1 \times 10^{-2} M_{\oplus} \text{ yr}^{-1}$. When this limiting rate is reached, the planet contracts inside its accretion radius, but is still assumed to be in hydrostatic equilibrium. The accreting gas is delivered hydrodynamically onto the planet at near free-fall velocities. This hydrodynamic arrival of nebular gas creates a shock at the upper boundary of the planet’s atmosphere. Regardless of its thermal energy, gas is presumed to be delivered homogeneously over the entire surface of the planet. In fact, since the gas is accreted from a circumplanetary disk, the morphology of accretion may be quite different. We do not consider such issues here, although they could be of some importance.

The treatment of mass and energy delivered through this shock (Stahler et al. 1980) is the single most important influence on the final thermal state of the planet. The gas is assumed to fall from the radius of the Hill sphere onto the shock, which lies at the upper boundary of the planetary atmosphere. To explore sensitivity to the thermal state of the pre-accreted gas, we computed a $2 M_J$ model with twice the assumed temperature for the nebular gas (300 instead of 150 K).

The precise luminosities expected from core accretion depend upon the assumed profile of the accretion rate, which is highly uncertain and in turn rests on assumptions about the ability of the nebula to supply gas to the planet. For these reasons, we do not place high confidence in the quantitative comparison of details of the early luminosity evolution between the various core accretion model masses. To explore the sensitivity of the evolution to the accretion rate, we computed models for $2 M_J$ with 1/10 and 10 times the baseline gas accretion rate, \dot{M}_{gas} . We do, however, regard with confidence the very large qualitative difference between planets that begin the isolation stage as relatively cool, low entropy objects and those which begin with the high entropy hot start as described in Section 3.3.

3. Evolution

We evolved each of the core accretion models to understand their thermal evolution subsequent to their formation. In principle, the core accretion planet formation code could be used to follow the subsequent cooling of each model planet. However, the grain-laden atmospheres that are incorporated into the formation calculation are not relevant after accretion ceases, when only relatively condensate-free gasses, mixed upwards from deeper in the atmosphere, are relevant. Thus, once the planet is fully formed we switch over to our fully non-gray EGP/brown dwarf atmosphere code in order to follow the planet’s subsequent evolution. In this section we explain precisely how we compute this evolution as well as our ‘hot start’ evolution to which we compare results.

3.1. Initial Conditions for Cooling

Our planetary evolution code has previously been applied to the cooling and contraction of Jupiter and Saturn (Fortney & Hubbard 2003), cool EGPs (Fortney & Hubbard 2004), and hot Jupiters (Fortney et al. 2006). To begin the calculation, we employ the envelope model at the termination of accretion from the core accretion code as the starting model for the subsequent evolution calculation. In the predominantly H/He envelope, we sample the deep convective interior to determine the specific entropy (S) of the planetary adiabat. We then construct a model planet with this same specific entropy (shown in Figure 2) for the start of the evolution phase. This ensures that the envelope has the same pressure/temperature/density profile at this boundary. Both the formation and evolution codes use the H/He EOS of Saumon et al. (1995) with $Y=0.243$. One structural change that we do make is in the core. While the formation code assumes a uniform core density of 3.2 g cm^{-3} , the evolution code uses the ANEOS equation of state for olivine (Thompson 1990), which allows for the expected significant compression of the core material. The core mass remains the same, but the core radius is substantially smaller in the evolution phase of the calculation³. However, the exact structure of the core has little effect on the evolution, especially for masses $\geq 2 M_J$, because the core is but a small fraction of the planet’s mass.

Our transition from formation to subsequent evolution involves a change in the outer boundary condition as well. During the formation phase, the outer boundary is appropriate for a planet embedded in the nebula, but during the evolution phase, the outer boundary

³We do not account for the gravitational potential energy that would be released if the core were to actually shrink.

condition is that of an isolated planet.

3.2. Atmospheric Boundary Condition

We employ a grid of non-gray radiative-convective atmosphere models to compute the evolution of giant planets and brown dwarfs. This grid relates the specific entropy of the adiabatic planetary interior (S) and surface gravity (g) to the planetary atmosphere’s effective temperature, T_{eff} , through a relation $T_{\text{eff}} = f(g, S)$. (Here S is parameterized as T_{10} , the temperature the adiabat would have at a pressure of 10 bar.) Saumon et al. (2006) have computed a cloud-free grid of atmospheres from $T_{\text{eff}} = 500\text{--}2400$ K and $\log g = 3.5\text{--}5.5$ cm sec⁻². We have computed ~ 75 additional model atmospheres to extend this grid down to $T_{\text{eff}}=90$ K and $\log g = 1.0$, to cover the lower effective temperatures and gravities necessary to study the evolution of 1 to 10 M_{J} planets. The assumption of cloud-free atmospheres is valid here, because, as we show below, effective temperatures for these planets cluster around 500–800 K at young ages, while water cloud condensation should not begin until $T_{\text{eff}} < 500$ K (Burrows et al. 2003).

The atmosphere code has previously been implemented for a variety of planetary and substellar objects. Applications include the generation of pressure-temperature (P – T) profiles and spectra for Titan (McKay et al. 1989), brown dwarfs (Marley et al. 1996; Burrows et al. 1997; Marley et al. 2002; Saumon et al. 2006), Uranus (Marley & McKay 1999), and hot Jupiters (Fortney et al. 2005b, 2006). The radiative transfer solving scheme is described in Toon et al. (1989). We use the elemental abundance data of Lodders (2003) and compute chemical equilibrium compositions following Fegley & Lodders (1994), Lodders & Fegley (2002), and Lodders (2002). The large and constantly updated opacity database is described in R. S. Freedman and K. Lodders (2007, in prep.).

3.3. Hot Start Models

To compare the evolution calculations employing the core accretion models as the initial condition to the type of evolution models primarily represented in the literature, we computed a second set of models employing what we term a “hot start.” These models assume that the planet, at all ages, has reached its final mass and possesses a fully adiabatic interior. An initial model is chosen with a high specific entropy adiabat (see Figure 2), corresponding to high internal temperatures. Our choices for initial entropy are very similar ($< 10\%$ difference) to those employed by Burrows et al. (1997). The heat extracted from the planet’s interior

per unit mass is given by:

$$\frac{\partial L}{\partial m} = -T \frac{\partial S}{\partial t}, \quad (1)$$

where L is the planet’s intrinsic luminosity, T is the temperature of a mass shell, S is the specific entropy of a mass shell, and t is the time. At the start of an evolutionary sequence L is large, so the time steps ∂t are consequently small. We note that cooling curves can be constructed back to an arbitrarily young age with this procedure, although authors such as Burrows et al. (1997), Chabrier et al. (2000), Baraffe et al. (2003b), who utilize this technique because of its convenience, typically only plot evolution for ages $> 10^6$ years, with the notion that the evolution at younger ages with this formalism probably does not correspond to reality. With our own “hot start” models, we reproduce well the results of Burrows et al. (1997) and Baraffe et al. (2003b) for the early evolution of 1 to 10 M_J planets; those authors used cloud-free atmosphere models similar to the ones we use here.

The thermal time scale, τ , of the evolving planet is roughly given by the Kelvin-Helmholtz time scale,

$$\tau \approx \frac{GM^2}{RL}, \quad (2)$$

where G is the gravitational constant, M is the mass of the planet, and R is the radius of the planet. Since the hot start planets have much larger initial L and R , their initial cooling rate is correspondingly faster than that of the core accretion planets. Since both the hot start and core accretion evolution tracks utilize the same atmospheric boundary conditions and model approach, any difference between the two must be attributable to the different initial conditions.

4. Discussion

4.1. Luminosity, Mass, and Radius of Young Planets

By combining our extension of the protoplanetary accretion calculation described in Hubickyj et al. (2005) with our calculation of the subsequent evolution, we produce models of the evolution of luminosity, radius, effective temperature (T_{eff}) of the planet with time. Our results are shown in Figures 3 and 4 which compare the core accretion evolutionary tracks to the conventional ‘hot-start’ scenario.

At very young ages, while a planet is still forming, the luminosity is of course far lower than the hot-start case where the planet is assumed to instantaneously form at time $t = 0$. During runaway gas accretion (around 2.5 Myr), the luminosity, which is almost entirely derived from the accretion shock, peaks in the range of 0.1 to 0.01 L_{\odot} (solar luminosity),

although the precise value is highly dependent on the assumed limiting gas accretion rate and the shock physics. A planet caught during this time period would be brighter than at any other time during its evolution.

As gas accretion is turned off in the core accretion case, the luminosity rapidly collapses to between 10^{-5} to $10^{-6} L_{\odot}$, depending upon the mass. At this point, the more massive planets have lower entropies (Figure 2), because a proportionately greater amount of their mass has passed through the shock and arrives with low entropy. As a result, post-accretion luminosity decreases with increasing mass (Figure 3), a result that is entirely a consequence of our treatment of the accretion shock. With the lowest gravity, the $1 M_J$ planet has the largest radius (Figure 3) and the highest post-formation luminosity.

The ‘hot-start’ models begin with arbitrarily large initial luminosities, greater than $10^{-4} L_{\odot}$, that expeditiously decay away. Since these planets start fully formed, the choice of time $t = 0$ for comparison to the core accretion models is somewhat arbitrary. In Figure 3, we equate the time of the first hot-start model to time $t = 0$ for the core accretion model. This allows the hot-start models a 2 to 3 million year ‘head start’ in their cooling and consequently minimizes the difference from the core accretion predicted luminosity. Nevertheless, with the sole exception of the $1 M_J$ planet, all of the model core-accretion model planets are *substantially fainter* immediately after the end of accretion than the comparable hot start model at the same age. A $10 M_J$ model is over two orders of magnitude fainter than if it experienced a hot start. The difference in L falls with mass, reaching a factor of two for a $2 M_J$ model. The $1 M_J$ planet formed by core accretion is a factor of two brighter than produced by the equivalent hot start.

In Figure 4 we set time $t = 0$ for the hot-start evolution to coincide with the first post-formation core accretion model. In this case, which maximizes the difference between the two approaches, the hot-start luminosity is larger for every planet mass, although the difference is again least for the lowest mass case. As illustrated in this figure, the lower initial entropy of the core accreted planets manifests as both a smaller initial radius and a much smaller effective temperature, both of which lead to a smaller luminosity. The hot start evolution predicts that the most massive models at 1 Myr have a radius over twice that of Jupiter’s and an effective temperature exceeding 2000 K. By contrast, the core accretion calculation predicts $R < 1.5 R_J$ and $T_{\text{eff}} < 900$ K for all cases.

Note that as the post-core accretion luminosity falls very slowly, the curves almost seem flat on the log-log plot. This is because the small, cool, core accretion planets cool far more slowly than the large, bright, hot-start planets (see Eq. 2).

A test of giant planet formation models is provided by the transiting hot Jupiters. It is

commonly postulated that the evolution of these planets is retarded when they arrive close to their parent star, since their thermal emission and atmospheric structure are dominated by the vast incident radiation (see the review by Charbonneau et al. (2006)). Given its anomalously large radius of $1.320 \pm 0.025 R_{\text{Jup}}$ (Knutson et al. 2006) for its mass of $0.66 \pm 0.06 M_{\text{Jup}}$, some have suggested that an additional source of energy (also related to the proximity of the primary) may be helping to delay the contraction of the transiting planet HD 209458 b. Regardless of whether such a source exists—and assuming that the planet never grew in size—the large radius sets a lower limit to acceptable post-accretion radii for this planet. As Figure 4 shows, the post-formation core accretion radius increases with falling mass and an isolated $1 M_{\text{J}}$ planet exceeds the observed radius of HD209458 b for over 10^7 years, allowing plenty of time for the planet to migrate to its current position (Papaloizou et al. 2006). Thus the radius HD209458 b seems to be consistent with our core accretion model (although we did not compute a model for this precise mass). Furthermore, our implementation of core accretion predicts that all non-accreting planets have radii less than $\sim 1.4 R_{\text{J}}$, since the model radii of massive core-accreted planets are never larger than this value and their evolution cannot be halted at a larger size. In contrast, a migrating, massive hot start planet could conceivably have a radius in excess of $1.6 R_{\text{J}}$ if its evolution were retarded early enough.

4.2. Subsequent Evolution

If infant core accreted Jupiters are fainter than their hot start cousins, for how long does the disparity persist? Figure 4 shows that by 10^7 yr the luminosity of a core accreted Jupiter is essentially identical to that of a hot start planet. Since the initial luminosity disparity is greater with increasing mass, it is no surprise that more massive core accreted planets take longer to match the hot start prediction. However, the timescale required is much larger than generally appreciated. A $2 M_{\text{J}}$ planet takes almost 10^8 year to match the hot start track. A $10 M_{\text{J}}$ planet requires a full 10^9 year to overcome its initial luminosity deficit.

Baraffe et al. (2002) also evaluated the uncertainty in the early evolution of brown dwarfs and giant planets by comparing what might be termed ‘hot start’ and ‘hotter start’ models. Both are comparable to our ‘hot start’ case, for example for their $5 M_{\text{J}}$ evolution the initial effective temperature was greater than 2000 K for both cases. Not surprisingly (see Eq. 2), they found that their hotter models with even larger initial radii cooled very quickly and joined their ‘hot start’ evolution tracks within a million years for all masses considered ($> 5 M_{\text{J}}$). This was the basis for their expressed confidence that the theoretical evolution tracks can be trusted for ages greater than a few million years. Motivated by a

preliminary report of our work (Fortney et al. 2005a), Chabrier et al. (2006) also briefly considered the early evolution of cool 1 and 4 M_J planets with small initial radii. They also found that smaller, cooler planets can take in excess of 10^7 years to reach the standard hot-start luminosity tracks.

To illustrate the extreme sensitivity of the early cooling rate on initial entropy, we computed the Kelvin-Helmholtz cooling times for a 4 M_J planet with a variety of initial internal entropies. For S (expressed in units of k_B /baryon) between 6 and 11, a range that more than spans the plausible initial entropies shown in Figure 2, we found that $\tau_{\text{HK}} \propto e^{-2.8S}$. Thus small changes in the initial estimate of S produce disproportionately large changes the initial cooling rate. Large values of S yield fast cooling rates, and the rapid cooling rates led to the conventional wisdom that planets rapidly forget their initial conditions. But smaller values of S , which our implementation of the core accretion model predicts, yield much slower early cooling times and planets with longer memories.

For this reason, as we noted in Section 2.2, we do not place high confidence in the comparison between individual early evolution tracks for core accreted planets of different masses, because they differ from each other relatively little in initial S . *The details of the accretion shock and the mass accretion rate and timescale, which are essentially unknown, control S and the relative initial post-accretion luminosity to a much greater degree than previously recognized.* In any case, for masses $\gtrsim 4 M_J$, there is relatively little difference in the luminosity among the core accreted giant planets until about 30 to 50 million years after formation. As a whole, our core accreted planets have substantially lower initial entropies and thus longer evolution times than the hot start models. We plan to explore the early post-formation luminosity evolution of the core accreted planets, including the effects on satellites, in more detail in a future publication.

4.3. Sensitivity to Assumptions

To understand the sensitivity of the results to the limiting gas accretion rate we varied both the maximum gas accretion rate and the timescale for accretion cutoff during accretion phases 4 and 5, for a 2 M_J planet. Results are shown in Figure 5. In the rapid gas accretion case, where the limiting accretion rate is set at $10^{-1} M_{\oplus} \text{yr}^{-1}$, the final planet is formed very quickly, in less than 10^5 yr after the start of runaway gas accretion. The resulting planet is somewhat larger and warmer than the baseline model. Likewise a model with a very low accretion rate, $10^{-3} M_{\oplus} \text{yr}^{-1}$, and a long accretional tail off ends up cooler and smaller than the baseline case. By 5 Myr, however, the differences between these cases are slight, less than 20% in the total luminosity, much less than the factor of 2 difference between the core

accretion and hot start models for this mass. We also considered a case for $10 M_J$ where we shortened, by a factor of 3, the time scale over which the accretion rate is linearly decreased from the limiting rate to zero. Except for reaching the final mass more rapidly, this model behaved identically to the standard case and is not shown.

Varying the temperature of the nebular gas, from 150 K to a very high 300 K, delays the onset of runaway gas accretion and alters the final thermal state of the planet, but the luminosity difference is within the range found by only varying the mass accretion rate. As shown in Figure 2, these relatively large changes in the nebular conditions for core accretion mechanism produce only slight differences in the initial entropy of the planet, which is the quantity that controls the subsequent evolution.

4.4. Masses of Young Giant Planets

Since young giant planets of known ages and dynamically-constrained masses have not yet been directly detected, the predictions of our model cannot yet be tested. However young, planetary mass companions are now being discovered and characterized. We find it is illuminating to explore some of the properties of these objects—although they almost certainly formed by fragmentation and not core accretion—in light of our new understanding of the sensitivity of the evolution models to initial conditions.

The companion to 2MASS1207 (Chauvin et al. 2005; Song et al. 2006) has an estimated luminosity of $\log(L/L_\odot) \approx -4.30$ at an age of 8 ± 3 Myr. Judging from the hot start evolution tracks shown in Figure 6, a mass of about 3 to $7 M_J$ is reasonably inferred, consistent with the $5 \pm 3 M_J$ reported by Song et al. (2006). However, as we have seen, at such a young age, the model luminosities are highly dependent on the initial entropy of the evolution tracks. Without a model connecting the formation process of these objects to their initial entropy, the model-dependent uncertainty in their masses is unconstrained.

To illustrate this point, we computed (Fig. 6) two evolution tracks, for 4 and $10 M_J$ planets, with initial entropies between the hot start and our core accretion cases. The initial conditions were chosen such that the entropy at 1 Myr would be equal to the mean the other two cases at an age of 1 Myr. Clearly if 2MASS1207b experienced such a ‘warm start’, the derived mass would be closer to $8 M_J$ than to $5 M_J$. While we make no claim to the applicability of such an arbitrary model to this particular object, we stress that until the model evolutionary curves can be calibrated at young ages, the derived masses are highly uncertain. Even these intermediate ‘warm start’ models take 20 to 100 Myr to reach the standard model curves, a time span that still is substantially longer than the age of many

young clusters.

This point is further illustrated by a second putative planetary mass object, GQ Lup b (Neuhäuser et al. 2005). Judging by our baseline hot-start luminosity tracks, this object has a mass in excess of $10 M_J$. Lower initial model entropies would result in higher estimated masses. Using a different set of models, with presumably higher initial entropies, the discoverers claimed a lower mass limit of $1 M_J$. Neuhäuser et al. (2005) arrived at their low mass estimate by relying on evolution models of Wuchterl & Tscharnuter (2003) that attempt to connect the initial conditions to the formation process, which is clearly a topic that requires more attention.

Indeed, the question of what is the proper initial condition to use in evolution models of giant planets and stars is an old one. Bodenheimer (1974) recognized that the choice of a giant planet’s final state after accretion would affect subsequent evolution. Observations of the thermal emission of young planets with dynamically constrained masses and known ages will shed light on the nature of the giant planet formation process, particularly the role of the accretion shock.

5. Conclusions

We have computed the first giant planet evolution models that couple planetary thermal evolution to the predicted core mass and thermal structure of a core accretion planet formation model. Baraffe et al. (2006) investigated the evolution of planets with core sizes and heavy element abundances derived from the core accretion models of Alibert et al. (2005). However, Baraffe et al. (2006) did not attempt to match the thermal structure (and hence, temperature, entropy, and density) at the interface between planetary formation and subsequent evolution.

Our implementation of the core accretion model processes most of the planetary mass through an accretion shock in which the accreting gas loses most of its internal entropy. As a result, our young giant planets are cooler, smaller, fainter, and take longer to evolve than the standard hot-start model giant planets. We note, however, that our accretion model does not resolve the radiative transfer within the shock, but rather uses the shock boundary conditions of Stahler et al. (1980). A more complete or detailed treatment of accretion at the surface of the planet could very well result in different initial conditions, including possibly a warmer, larger, brighter and more conventional young planets. Specifically, a three-dimensional hydrodynamic simulation of gas accretion by giant planets, allowing for material accreted through a circumplanetary disk and shock radiation, would provide more

rigorous post-formation models for subsequent evolution calculations. Until such models are available, our approach—which likely provides a lower limit to the post accretion luminosity—demonstrates that plausible initial conditions can lead to very different early evolution tracks for giant planets than the ‘hot start’ models that are commonly relied upon.

For example, at 10^7 years—a time greater than the age of the TW Hydrae association—our $10 M_J$ core accreted planet is more than a factor of 100, or 5 magnitudes, fainter than the equivalent hot start planet. The luminosity difference falls with decreasing mass, so that our model luminosity for a $1 M_J$ planet is comparable to the standard case. Thus the thermal luminosity of young, massive giant planets, which have been assumed to be easy targets for coronagraphy, may be substantially less than previously assumed. If this result is correct, then searches for the thermal emission from young, several Jupiter mass planets must be far more sensitive than previously anticipated in order to detect these relatively faint, young planets. Thermal infrared planet searches by the Large Binocular Telescope, the James Webb Space Telescope, and other planned telescopes would all be impacted, although efforts to detect planets in reflected light would not. This conclusion holds true even to ages as great as that of the Pleiades for the most massive planets considered here. Ironically the least massive, most intrinsically faint planets (1 to $2 M_J$) match their hot-start luminosity tracks by just a few tens of millions of years, or less and are much less underluminous before that time. Direct detections of young giant planets with dynamically measured masses will test this conclusion.

Since the numerical values for luminosity that we derive depend primarily upon our treatment of energy radiated from the accretion shock, these results should not be viewed as specific predictions of the core accretion model. Rather our point is that core accretion naturally leads to gas accretion through a shock, which may result in low entropy planets. The viability of giant planet formation via core accretion depends on physical processes happening earlier in the accretionary process (at smaller masses) than those processes that we have shown to be crucial for the luminosity of young planets of Jupiter’s mass and larger.

We note in passing that the faintness predicted for young Jupiter-mass planets compounds with non-equilibrium chemistry to make detection of young giant planets at M band particularly challenging. Marley et al. (1996), after the discovery of G1229B, suggested that a substantial M-band $4 - 5 \mu\text{m}$ flux peak should be a universal feature of giant planets and brown dwarfs. In addition to the intrinsic emergent flux, this spectral range has looked promising for planet detection due to the favorable planet/star flux ratio (e.g. Burrows 2005). However, it has been known since the 1970s (see Prinn & Barshay 1977) that Jupiter’s $5 \mu\text{m}$ flux is suppressed by absorption by CO present in amounts exceeding that predicted by equilibrium chemistry. This same effect has now been observed in brown dwarf M-band

photometry (Golimowski et al. 2004; Leggett et al. 2006), as anticipated by Fegley & Lodders (1996). Excess CO leads to strong absorption at $4.5 \mu\text{m}$, leading to diminished flux in M-band (Saumon et al. 2003). This effect further suppresses the M band fluxes of young planets below the existing models. Taken together, fainter young planets and reduced M-band flux may well reduce the catch from what had seemed a promising fishing hole for direct planet detection.

We also conclude that the predicted evolution of giant planets objects, regardless of formation mechanism, is far more sensitive to the precise conditions at the termination of accretion than has been previously recognized. Most workers have assumed that evolving model planets ‘forget’ their initial conditions within 10^6 (Baraffe et al. 2003a) to 10^8 years (Stevenson 1982) of the first time step. While 1 to 2 Jupiter mass planets do have a short ($\sim 10^7$ yr) memories, we have shown that more massive planets remember their initial thermal state far longer. The evolution time scale for young, hot planets depends exponentially on their initial entropy. Until the initial thermal state of young, low mass objects—even isolated brown dwarfs—is known with more certainty, the early evolution tracks must be regarded with some skepticism. Any effort to assign a mass to a very young putative giant planet must consider the uncertainties in these early evolutionary tracks.

We acknowledge support from the NASA Origins and Planetary Atmospheres Programs, from the NSF Astronomy and Astrophysics Program, and from a NASA Postdoctoral Program (NPP) Fellowship (J. J. F.). We thank Richard Freedman and Katharina Lodders for assistance with molecular opacities and chemistry, respectively. We benefited from helpful exchanges with Günther Wuchterl and a helpful review by the anonymous referee.

REFERENCES

- Alibert, Y., Mordasini, C., Benz, W., & Winisdoerffer, C. 2005, *A&A*, 434, 343
- Baraffe, I., Alibert, Y., Chabrier, G., & Benz, W. 2006, *A&A*, 450, 1221
- Baraffe, I., Chabrier, G., Allard, F., & Hauschildt, P. 2003a, in *IAU Symposium 211*, ed. E. Martín, 41
- Baraffe, I., Chabrier, G., Allard, F., & Hauschildt, P. H. 2002, *A&A*, 382, 563
- Baraffe, I., Chabrier, G., Barman, T. S., Allard, F., & Hauschildt, P. H. 2003b, *A&A*, 402, 701

- Bodenheimer, P. 1974, *Icarus*, 23, 319
- Bodenheimer, P. 1976, *Icarus*, 29, 165
- Bodenheimer, P., Grossman, A. S., Decamp, W. M., Marcy, G., & Pollack, J. B. 1980, *Icarus*, 41, 293
- Bodenheimer, P., Hubickyj, O., & Lissauer, J. J. 2000, *Icarus*, 143, 2
- Bodenheimer, P. & Pollack, J. B. 1986, *Icarus*, 67, 391
- Boss, A. P. 1998, *ApJ*, 503, 923
- Burrows, A. 2005, *Nature*, 433, 261
- Burrows, A., Hubbard, W. B., Lunine, J. I., & Liebert, J. 2001, *Reviews of Modern Physics*, 73, 719
- Burrows, A., Marley, M., Hubbard, W. B., Lunine, J. I., Guillot, T., Saumon, D., Freedman, R., Sudarsky, D., & Sharp, C. 1997, *ApJ*, 491, 856
- Burrows, A., Sudarsky, D., & Lunine, J. I. 2003, *ApJ*, 596, 587
- Chabrier, G., Baraffe, I., Allard, F., & Hauschildt, P. 2000, *ApJ*, 542, 464
- Chabrier, G., Baraffe, I., Selsis, F., Barman, T., Hennebelle, P., & Alibert, Y. 2006, *Protostars and Planets V*, in press
- Charbonneau, D., Brown, T., Burrows, A., & Laughlin, G. 2006, *Protostars and Planets V*, in press
- Chauvin, G., Lagrange, A.-M., Dumas, C., Zuckerman, B., Mouillet, D., Song, I., Beuzit, J.-L., & Lowrance, P. 2004, *A&A*, 425, L29
- . 2005, *A&A*, 438, L25
- Fegley, B. J. & Lodders, K. 1994, *Icarus*, 110, 117
- . 1996, *ApJ*, 472, L37
- Fortney, J. J. & Hubbard, W. B. 2003, *Icarus*, 164, 228
- . 2004, *ApJ*, 608, 1039
- Fortney, J. J., Marley, M. S., Hubickyj, O., Bodenheimer, P., & Lissauer, J. J. 2005a, *Astronomische Nachrichten*, 326, 925

- Fortney, J. J., Marley, M. S., Lodders, K., Saumon, D., & Freedman, R. 2005b, *ApJ*, 627, L69
- Fortney, J. J., Saumon, D., Marley, M. S., Lodders, K., & Freedman, R. S. 2006, *ApJ*, 642, 495
- Golimowski, D. A., Leggett, S. K., Marley, M. S., Fan, X., Geballe, T. R., Knapp, G. R., Vrba, F. J., Henden, A. A., Luginbuhl, C. B., Guetter, H. H., Munn, J. A., Canzian, B., Zheng, W., Tsvetanov, Z. I., Chiu, K., Glazebrook, K., Hoversten, E. A., Schneider, D. P., & Brinkmann, J. 2004, *AJ*, 127, 3516
- Graboske, H. C., Olness, R. J., Pollack, J. B., & Grossman, A. S. 1975, *ApJ*, 199, 265
- Grossman, A. S., Graboske, H., Pollack, J., Reynolds, R., & Summers, A. 1972, *Physics of the Earth and Planetary Interiors*, 6, 91
- Hubbard, W. B. 1980, *Reviews of Geophysics and Space Physics*, 18, 1
- Hubickyj, O., Bodenheimer, P., & Lissauer, J. J. 2005, *Icarus*, 179, 415
- Knutson, H., Charbonneau, D., Noyes, R. W., Brown, T. M., & Gilliland, R. L. 2006, *ApJin press*, *ArXiv Astrophysics e-prints*, arXiv:astro-ph/0603542
- Lada, E. A. & Lada, C. J. 1995, *AJ*, 109, 1682
- Leggett, S. K., Saumon, D., Marley, M. S., Geballe, T. R., Golimowski, D. A., Stephens, D., & Fan, X. 2006, *ApJin press*,
- Lissauer, J. J. & Stevenson, D. J. 2006, *Protostars and Planets V*, in press
- Lodders, K. 2002, *ApJ*, 577, 974
- . 2003, *ApJ*, 591, 1220
- Lodders, K. & Fegley, B. 2002, *Icarus*, 155, 393
- Luhman, K. L. & Steeghs, D. 2004, *ApJ*, 609, 917
- Marley, M. S. & McKay, C. P. 1999, *Icarus*, 138, 268
- Marley, M. S., Saumon, D., Guillot, T., Freedman, R. S., Hubbard, W. B., Burrows, A., & Lunine, J. I. 1996, *Science*, 272, 1919
- Marley, M. S., Seager, S., Saumon, D., Lodders, K., Ackerman, A. S., Freedman, R. S., & Fan, X. 2002, *ApJ*, 568, 335

- McKay, C. P., Pollack, J. B., & Courtin, R. 1989, *Icarus*, 80, 23
- Mizuno, H. 1980, *Progress of Theoretical Physics*, 64, 544
- Neuhäuser, R., Guenther, E. W., Wuchterl, G., Mugrauer, M., Bedalov, A., & Hauschildt, P. H. 2005, *A&A*, 435, L13
- Papaloizou, J. C. B., Nelson, R. P., Kley, W., Masset, F. S., & Artymowicz, P. 2006, *Protostars and Planets V*, in press
- Pollack, J. B., Hubickyj, O., Bodenheimer, P., Lissauer, J. J., Podolak, M., & Greenzweig, Y. 1996, *Icarus*, 124, 62
- Prinn, R. G. & Barshay, S. S. 1977, *Science*, 198, 1031
- Saumon, D., Chabrier, G., & van Horn, H. M. 1995, *ApJS*, 99, 713
- Saumon, D., Marley, M. S., Cushing, M. C., Leggett, S. K., Roellig, T. L., Lodders, K., & Freedman, R. S. 2006, *ApJ* in press, astro-ph/0605563
- Saumon, D., Marley, M. S., Lodders, K., & Freedman, R. S. 2003, in *Brown Dwarfs, Proceedings of IAU Symposium #211*, ed. E. Martin, (San Francisco: Astronomical Society of the Pacific), 345
- Song, I., Schneider, G., Zuckerman, B., Farihi, J., Becklin, E. E., Bessell, M. S., Lowrance, P., & Macintosh, B. A. 2006, *ArXiv Astrophysics e-prints*
- Stahler, S. W. 1988, *PASP*, 100, 1474
- Stahler, S. W., Shu, F. H., & Taam, R. E. 1980, *ApJ*, 241, 637
- Stassun, K. G., Mathieu, R. D., & Valenti, J. A. 2006, *Nature*, 440, 311
- Stevenson, D. J. 1982, *Planet. Space Sci.*, 30, 755
- Thompson, S. L. 1990, ANEOS—Analytic Equations of State for Shock Physics Codes, Sandia Natl. Lab. Doc. SAND89-2951
- Toon, O. B., McKay, C. P., Ackerman, T. P., & Santhanam, K. 1989, *Journal of Geophysical Research*, 94, 16287
- Webb, R. A., Zuckerman, B., Platais, I., Patience, J., White, R. J., Schwartz, M. J., & McCarthy, C. 1999, *ApJ*, 512, L63
- Wuchterl, G. 2005, *Astronomische Nachrichten*, 326, 905

Wuchterl, G. & Tscharnuter, W. M. 2003, A&A, 398, 1081

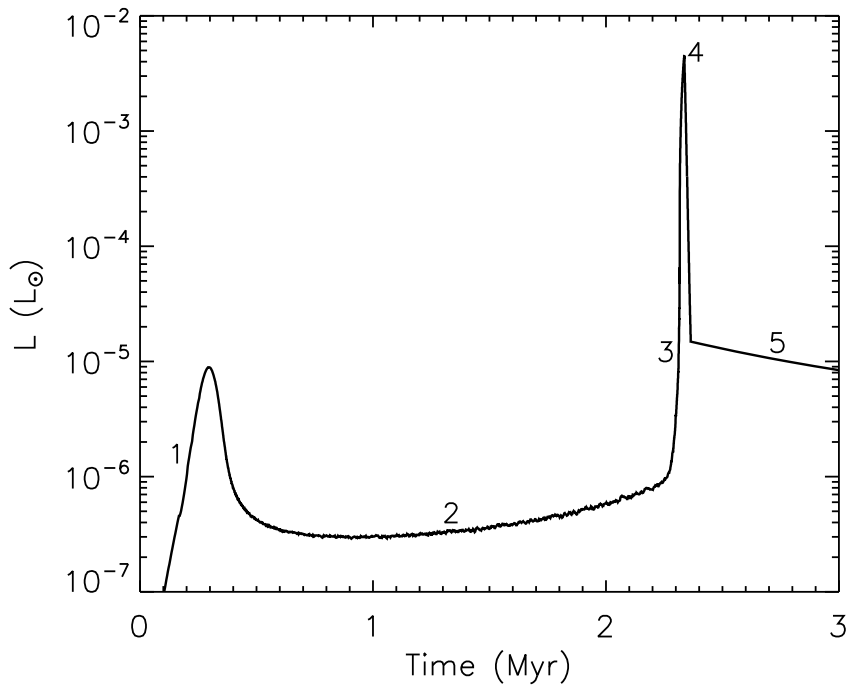


Fig. 1.— Luminosity of a $1 M_J$ planet as a function of time. Numbers refer to various stages in the formation/contraction process as discussed in the text. In this figure, time $t = 0$ is chosen to be the start of the growth of the solid core. Model, through stage 4, is the $10L_{\infty}$ case of Hubickyj et al. (2005). Subsequent evolution is calculated as described in Section 3.

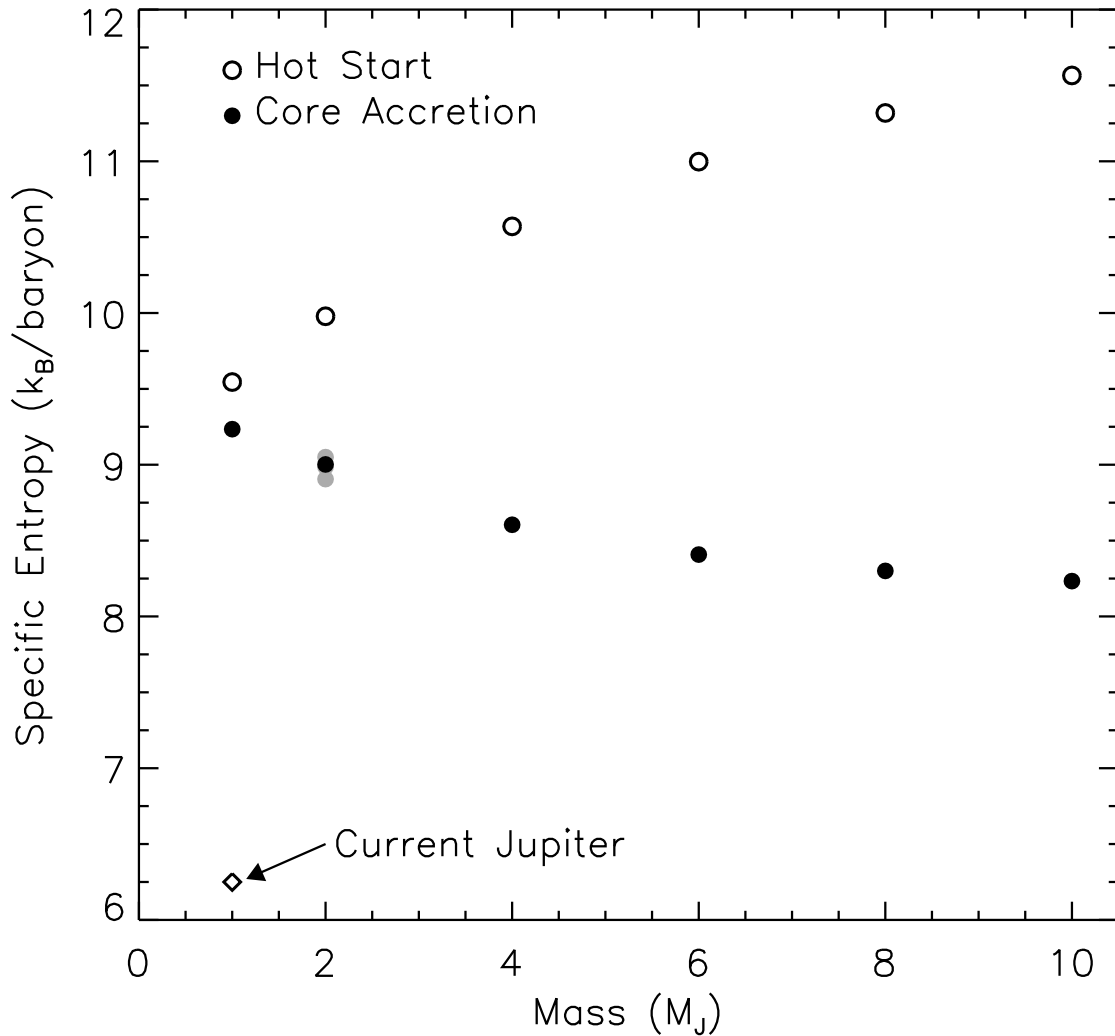


Fig. 2.— Specific entropy of young giant planets formed by core accretion and the hot-start assumptions. Since almost all of the mass of the planet sits on a single adiabat, the interior temperature-pressure conditions can be characterized by the entropy of that adiabat. For both cases the entropy plotted is at 1 million years after the first time step in the evolution model. Shaded circles at $2 M_J$ denote entropies of various alternate cases for the core accretion model, as shown in Figure 5 and discussed in Section 4.3. In the core accretion case this is 1 million years after the end of accretion. The entropy of the current Jupiter is also shown for comparison.

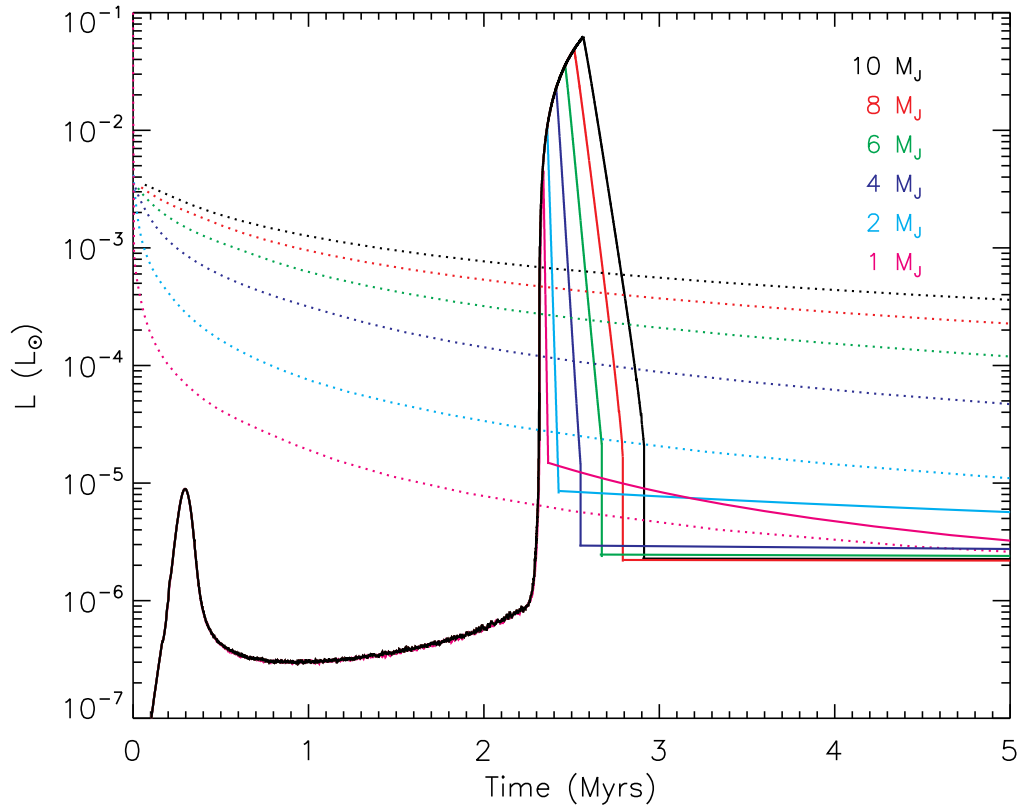


Fig. 3.— Luminosity of young Jupiters of various masses as a function of time. Dotted lines are for a ‘hot start’ evolution calculation as described in the text. Solid lines denote the core accretion case. In this figure, time $t = 0$ is chosen to be the start of the growth of the solid core for the nucleated collapse scenario and the first model of the ‘hot start’ evolution.

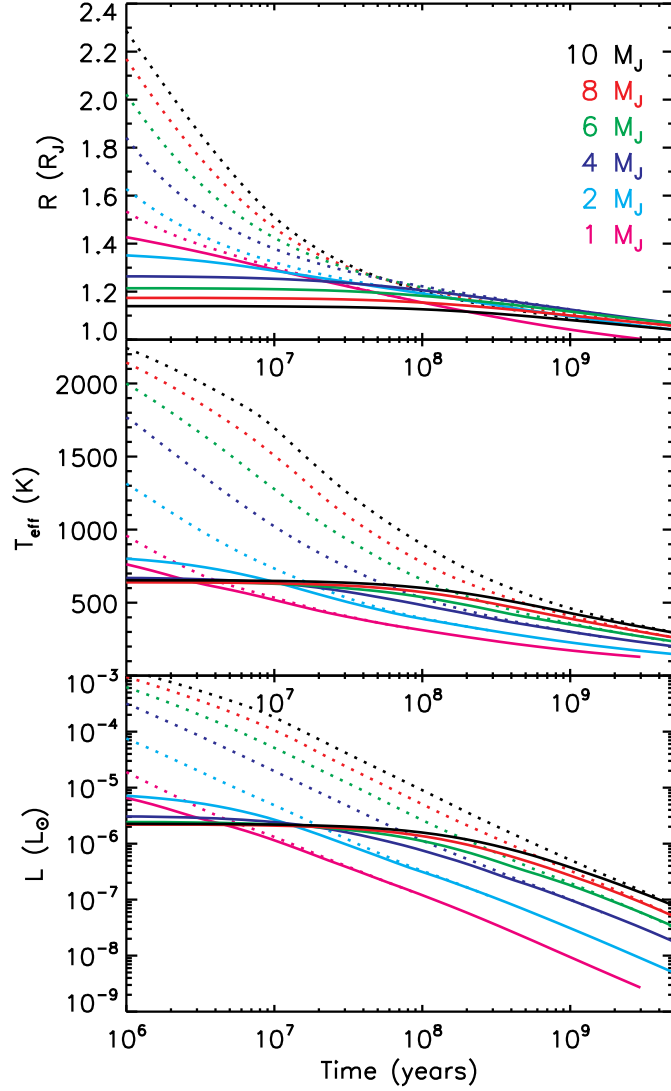


Fig. 4.— Model radius, R , effective temperature, T_{eff} , and luminosity, L , of young Jupiters of various masses. Line types as in Figure 2. Unlike Figure 2, in this figure time $t = 0$ for the core accretion evolution is chosen to be the last model of the core accretion calculation. There is thus an offset of 2.5 to 3 million years, depending on mass, from Figure 2. Both the radii and effective temperature of the young planets are lower in the core accretion case, leading to substantially lower luminosities. Differences from the ‘hot start’ persist for as little as 10^7 years for a $1 M_J$ planet to as much as 10^9 years for a $10 M_J$ planet.

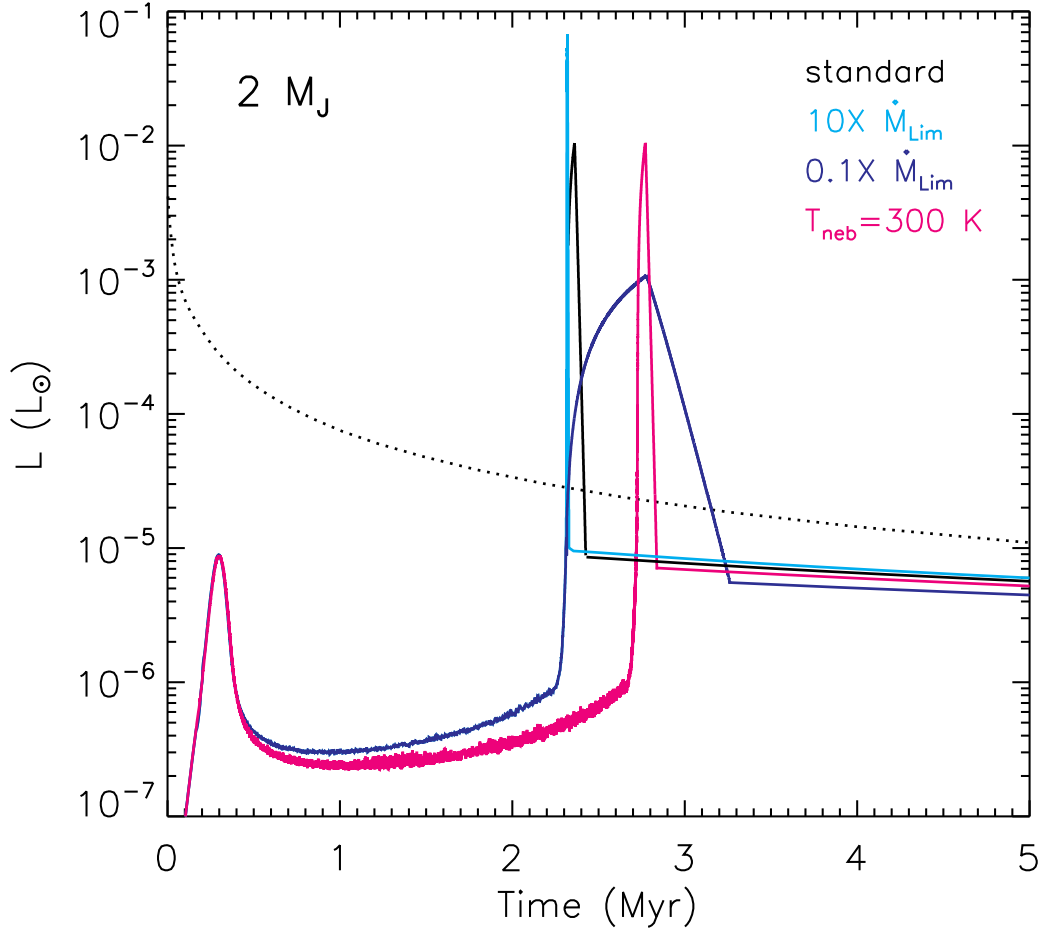


Fig. 5.— Luminosity evolution of various $2 M_J$ cases discussed in the text. Black solid and dotted lines are the standard baseline core accretion and hot start models. Other line types are for 10 and 0.10 times the standard limiting mass accretion rate, \dot{M}_{Lim} , and a case with higher nebular gas temperature, T_{neb} .

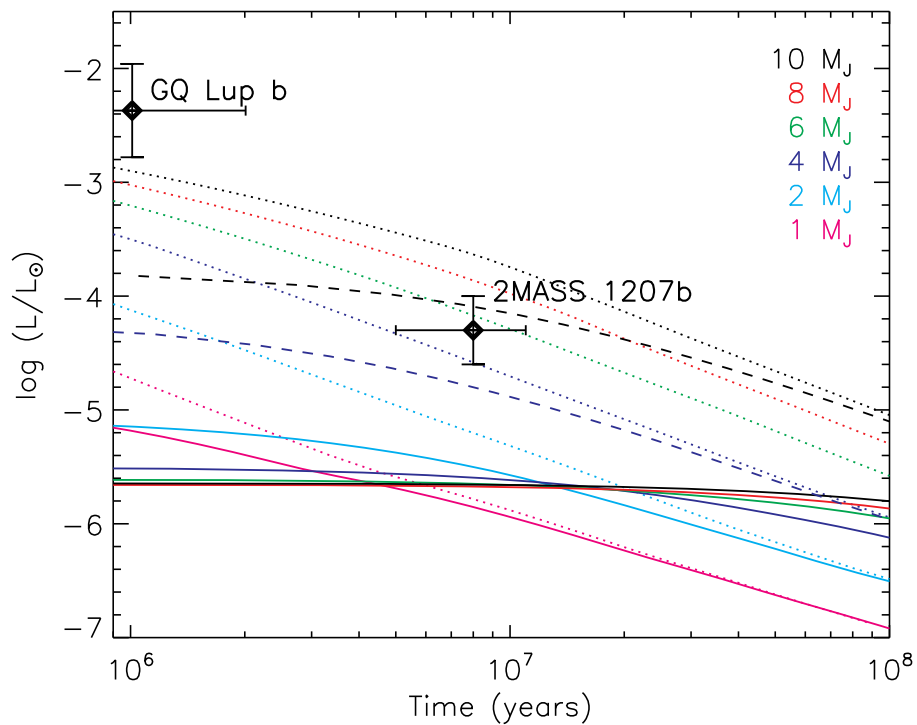


Fig. 6.— Luminosity evolution of various masses for the hot start (dotted), core accretion (solid), and intermediate entropy (dashed) cases. For the intermediate case, only tracks for the 4 and 10 M_J planets are shown. Also shown are the estimated (model dependent) bolometric luminosities of two claimed (Chauvin et al. 2005; Neuhäuser et al. 2005) giant planet mass companions to more massive objects.